

P-ISSN: 2706-7483  
 E-ISSN: 2706-7491  
 IJGGE 2023; 5(1): 151-161  
 Received: 21-12-2022  
 Accepted: 25-01-2023

**Aakriti Srivastava**  
 (1) Department of Earth  
 Science, Barkatullah  
 University, Bhopal,  
 Madhya Pradesh, India  
 (2) National Centre for Polar  
 and Ocean Research, Ministry  
 of Earth Sciences, Goa, India

**Dinesh Chandra Gupta**  
 Department of Earth Science,  
 Barkatullah University,  
 Bhopal, Madhya Pradesh,  
 India

**Avinash Kumar**  
 National Centre for Polar and  
 Ocean Research, Ministry of  
 Earth Sciences, Goa, India

**Corresponding Author:**  
**Aakriti Srivastava**  
 (1) Department of Earth  
 Science, Barkatullah  
 University, Bhopal,  
 Madhya Pradesh, India  
 (2) National Centre for Polar  
 and Ocean Research, Ministry  
 of Earth Sciences, Goa, India

## Estimation of ice shelf front changes using MODIS data and statistical approach

**Aakriti Srivastava, Dinesh Chandra Gupta and Avinash Kumar**

### Abstract

The Ronne ice shelf (RIS) dynamics and mass balance play key role to decipher changes in the global climate scenario. The spatio-temporal changes in ice shelf extent of the RIS were studied by dividing the study area into three sectors (I, II, III) and further into a number of transects at 5 km uniform intervals using multi-dated Moderate Resolution Imaging Spectro-radiometer (MODIS) satellite data (2004–2019) of the austral summer months (January–March). The average of rates (AOR), end point rate (EPR), and linear regression (LR) methods were used to estimate the rate of change in RIS extent. Based on the analysis, Sector II shows prominent changes, hence further detailed study has been carried out in this sector. The study reveals that the RIS extent has been prograded at the rate of 11 km/year to 26 km/year in 2019 with maximum increase of 26 km at TR63. Based on all the three methods, ice shelf extent shows a progradation in almost all transects. The RIS bounded by Lassiter coast (LC) and Berkner Island (BI) recorded advancement in the ice shelf extents which is the feedback of morphological features like ice rise, small inlets along the ice shelf. The present study demonstrates that the combined use of satellite imagery and statistical techniques can be useful in quantifying ice shelf morphological variability.

**Keywords:** Ronne ice shelf, Ice shelf extent, MODIS, progradation, statistical methods

### Introduction

An ice shelf is defined as a floating extension of land ice that plays an important role in glacier stability, ice sheet mass balance, ocean stratification and bottom water formation, especially through latent and sensible heat processes (Rignot *et al.*, 2013) [10]. The rate of change in ice shelves extent are controlled by the ocean-atmosphere temperatures adjacent to the ice shelves. An increase in ocean heat flux enhances the basal melting beneath ice shelves that leads to a loss of Antarctic ice sheet mass and contributes to sea-level rise. The continent of Antarctica is surrounded by ice shelves. These ice shelves cover more than 1.561 million km<sup>2</sup> (an area the size of Greenland), fringing about 75% of Antarctica's coastline, covering 11% of the total area and receiving 20% of its snow.

The ocean cavities beneath the ice shelves provides a temperature gradient across the ocean cavity through the pressure dependence of the freezing temperature and insulates the ocean cavity from atmospheric forcing (Webber *et al.*, 2017; Michael J M Williams *et al.*, 2001) [15, 17, 18]. The ocean circulation under the ice shelf is strongly linked to the forcing provided by the ice shelf and the bathymetry (Williams *et al.*, 2002) [19]. However, the presence of sea ice, indirectly modulates the stress on sea ice by reducing the amplitude of ocean swell (Thomson and Rogers, 2014) [13], and the freezing atmospheric temperatures thereby promote the changes in ice shelf morphology. The rate of melting and freezing at the interface between the ice shelf and the ocean can be characterized by the magnitude of the interaction between the ice shelf and the ocean. Hence, during the melting processes, the top layer of water column is cooled and freshened that tends to grade the top of the water column; whereas during freezing processes salinity increases due to salt release which tends to drive the convective mixing (Wen *et al.*, 2010; Michael J.M. Williams *et al.*, 2001) [16, 17, 18].

There are several studies have been carried out to understand its dynamic characteristics, such as ocean circulation under ice shelves (Hellmer and Jacobs, 1992; Herraiz-Borreguero *et al.*, 2015; Holland *et al.*, 2008; Michael J.M. Williams *et al.*, 2001) [5, 6, 7, 17, 18]; mapping the grounding zone (Fricker *et al.*, 2009, 2002) [3, 4] and ice sheet velocity (Joughin, 2002; King *et al.*, 2007; Walker *et al.*, 2015; Young and Hyland, 2002; Yu *et al.*, 2010) [8, 9, 14, 4, 21].

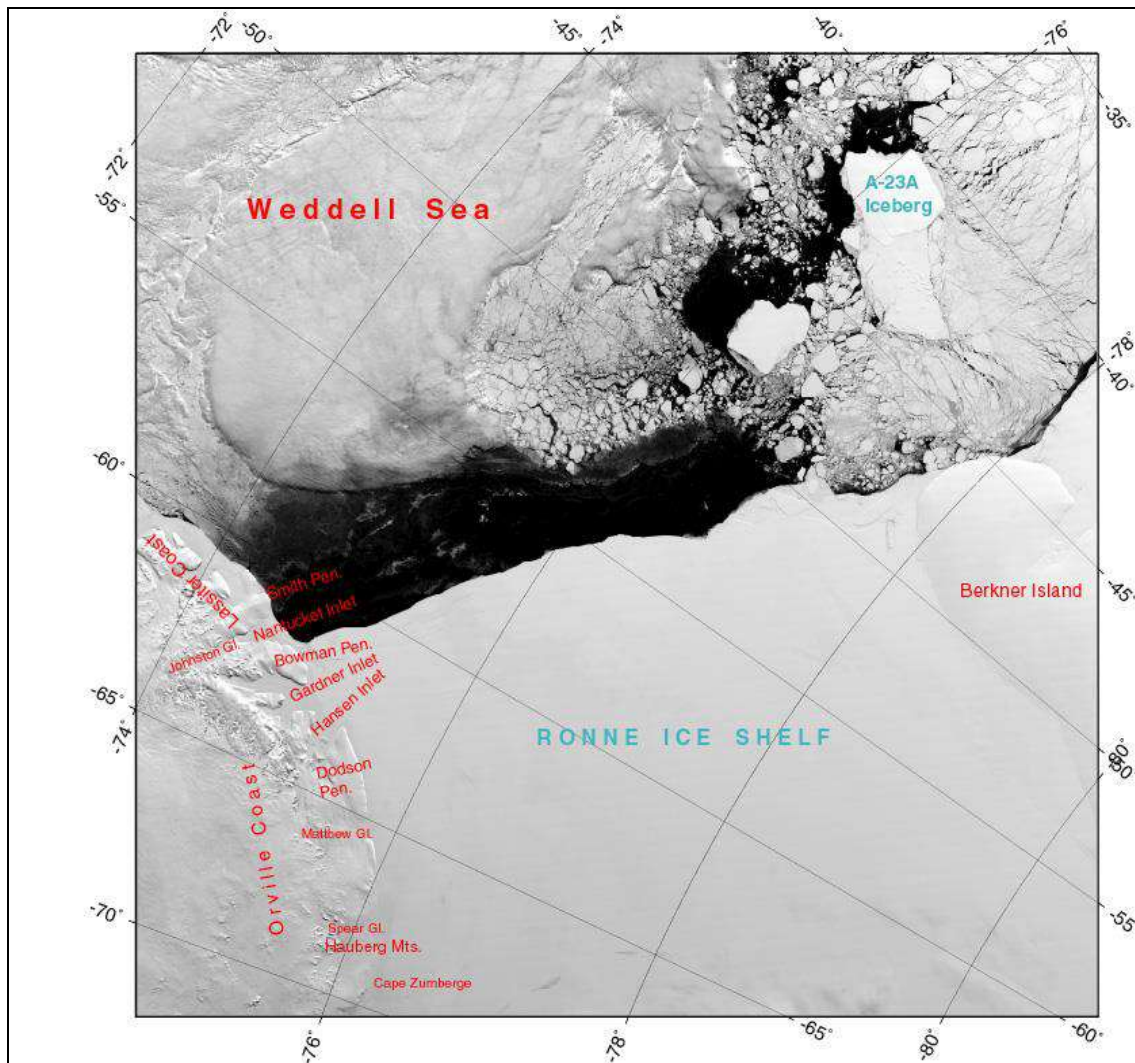


**Fig 1:** Map of Ronne Ice Shelf (Source: NSIDC)

### Study Area

Filchner-Ronne Ice Shelf is a large body of floating ice, that lies at the head of the Weddell Sea, that itself is an indentation in the Atlantic coastline of Antarctica. It covers more than 650 feet (200 m) thick and has an area of about 1,00,400 sq. miles (260,000 sq. km). The shelf extends inland on the eastern side of the Berkner Island that stretches for more than 250 miles (400 km) up to the escarpment of Pensacola Mountains. The name Filchner was originally given to the entire shelf, that includes the larger area lying to the west of Berkner Island now called the Ronne Ice Shelf. The Ronne ice shelf (RIS) is the larger and western part of the Filchner–Ronne ice shelf. It is bounded by Lassiter Coast (LC) on the west near Antarctic Peninsula and Berkner Island (BI) in the east (Rignot and MacAyeal, 1989) <sup>[11]</sup>. The study area on the eastern flank of the calving front contains Hemmen ice rise (HIR) and part of Berkner Island (BI) which is the largest ice rise in Antarctica (Swithinbank *et al.*, 2003) <sup>[12]</sup>

The Ronne Ice Shelf, has been named after Edit Ronne, who was the first American woman to visit Antarctica. She sat on the Weddell Sea, that lies just to the east of the Antarctic Peninsula and on the Transantarctic Mountains' rear slope. This huge ice shelf is the second largest in Antarctica and encompasses an area of about 1,70,660 sq. miles (422,000 sq. km). The Weddell Sea's deep blue water may be seen near the border of the ice sheet, while the remaining water is covered by floating ice.

The stability of the ice sheet is significantly influenced by the sea ice that surrounds the large Antarctic ice shelves. According to studies, the amount of salt released during the creation of sea ice during the autumn and winter transforms the water around and below the Ronne Ice Shelf into a kind of protective sheath. This saline water, which has an average temperature of minus 2 °C, aids in protecting the ice shelf from the milder seas delivered by the Weddell Gyre.

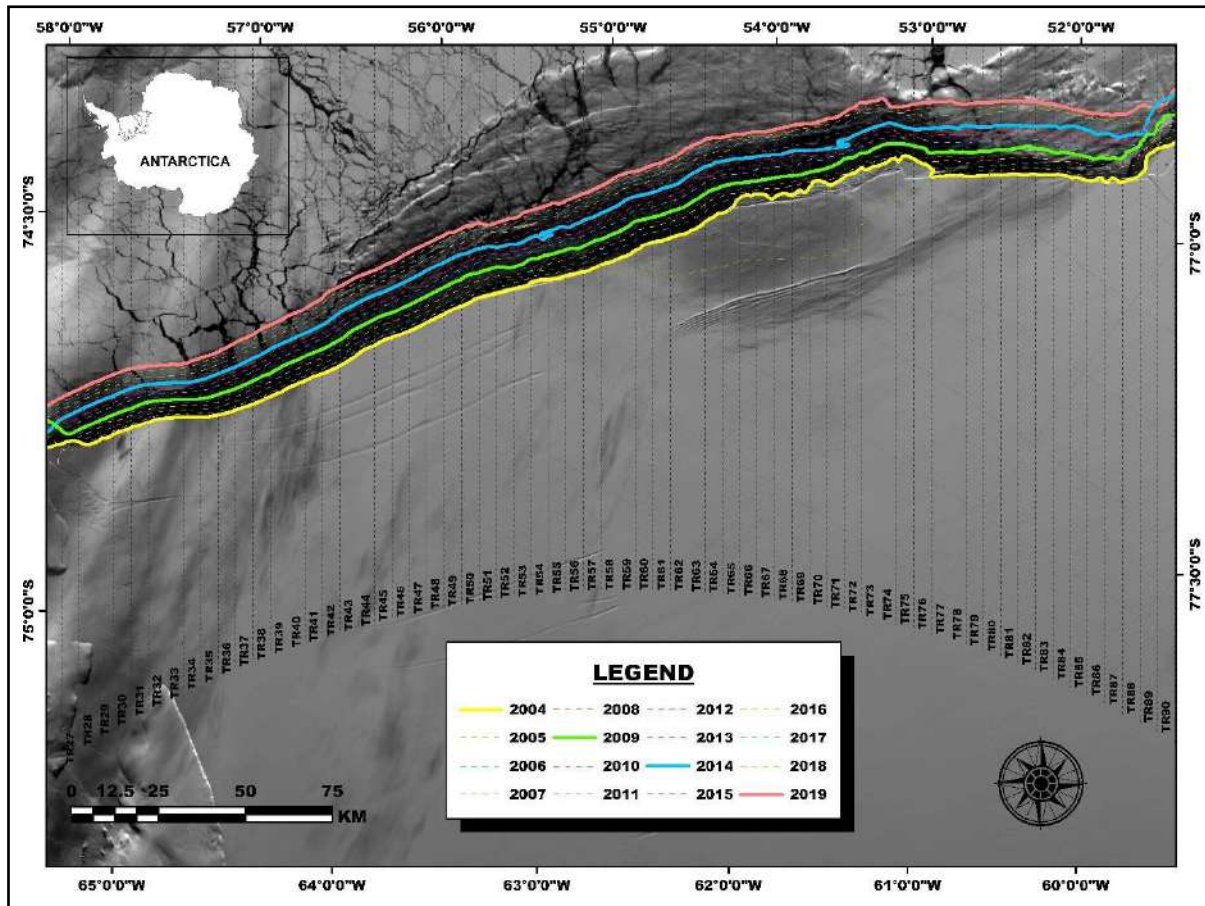


**Fig 2:** Study area map showing the Ronne Ice Shelf extent positions from 2004-2019, which has been divided into different transects (TR26 – TR91) at a 5 km uniform interval.

**Materials & Methods**

The spatio-temporal changes in the Ronne Ice Shelf have been analysed using cloud-free cover visible range of Moderate Resolution Imaging Spectro-radiometer (MODIS) satellite images for a period of 16 years, i.e., 2004 to 2019. The images have been downloaded from the archives of National Snow and Ice Data Center (NSIDC) website. The study has been done using the images from the austral

summer months (i.e., mid-February to early March). The study has been done during this period because the sea ice extent reaches its lowest with the annual ice shelf also being at its minimum extent. The images acquired from the [www.nsidc.org](http://www.nsidc.org) have been projected on the Polar Stereographic projection in order to determine the major ice shelf areas and its extent over the years. The data information and specifications have been given in Table 1.

**Table 1:** Details of the satellite data, specification and date of acquisition used for Ronne ice shelf extent delineation and analysis

Sensor/band specification/image type	Date of data acquisition
Moderate Resolution Imaging Spectroradiometer (MODIS) visible satellite data (250 m spatial resolution and wavelength of 620–876 nm). All the cloud-free image was acquired in Geo- tiff format	March 13 <sup>th</sup> , 2004; January 07 <sup>th</sup> , 2005; January 06 <sup>th</sup> , 2006; February 11 <sup>th</sup> , 2007; February 06 <sup>th</sup> , 2008; March 02 <sup>nd</sup> , 2009; March 02 <sup>nd</sup> , 2010; February 23 <sup>rd</sup> , 2011; February 19 <sup>th</sup> , 2012; March 16 <sup>th</sup> , 2013; February 06 <sup>th</sup> , 2014; February 27 <sup>th</sup> , 2015; March 08 <sup>th</sup> , 2016; March 02 <sup>nd</sup> , 2017; February 28 <sup>th</sup> , 2018; March 02 <sup>nd</sup> , 2019.

The ice water lines in the images have been demarcated and digitized by means of visual and digital interpretation on the ArcMap software. The study area has been found to cover a stretch of approximately 970 km. This digitized length has been divided into 150 transects at a uniform interval of 5 km vertical to the base year of 2004. The transects have been constructed to find out the difference in the extent of the ice shelf of each year from the base year 2004.

In order to understand the change better, the entire length has been divided into different sectors on the basis of the transects that have been drawn. The three sectors in which the area has been divided are: Sector I (TR1 to TR25), Sector II (TR26 to TR91) and Sector III (TR92 to TR150). For better visualization and understanding of the changes in

the ice shelf extent, the ice water line has been taken into consideration and digitized accurately. These vector layers have then been overlaid in order to detect the change better. The overlay analysis carried out on these layers have helped in estimating the amount of progradation and recession across the length of the ice shelf.

However, the main focus has been kept on Sector II of the ice shelf, as maximum change has been observed in that region. To find out the rate of change, three methods have been followed: End Point Rate, Average of Rates and Linear Regression methods. The computation for these methods has been done on MS-Excel and values is mentioned in Table 2.

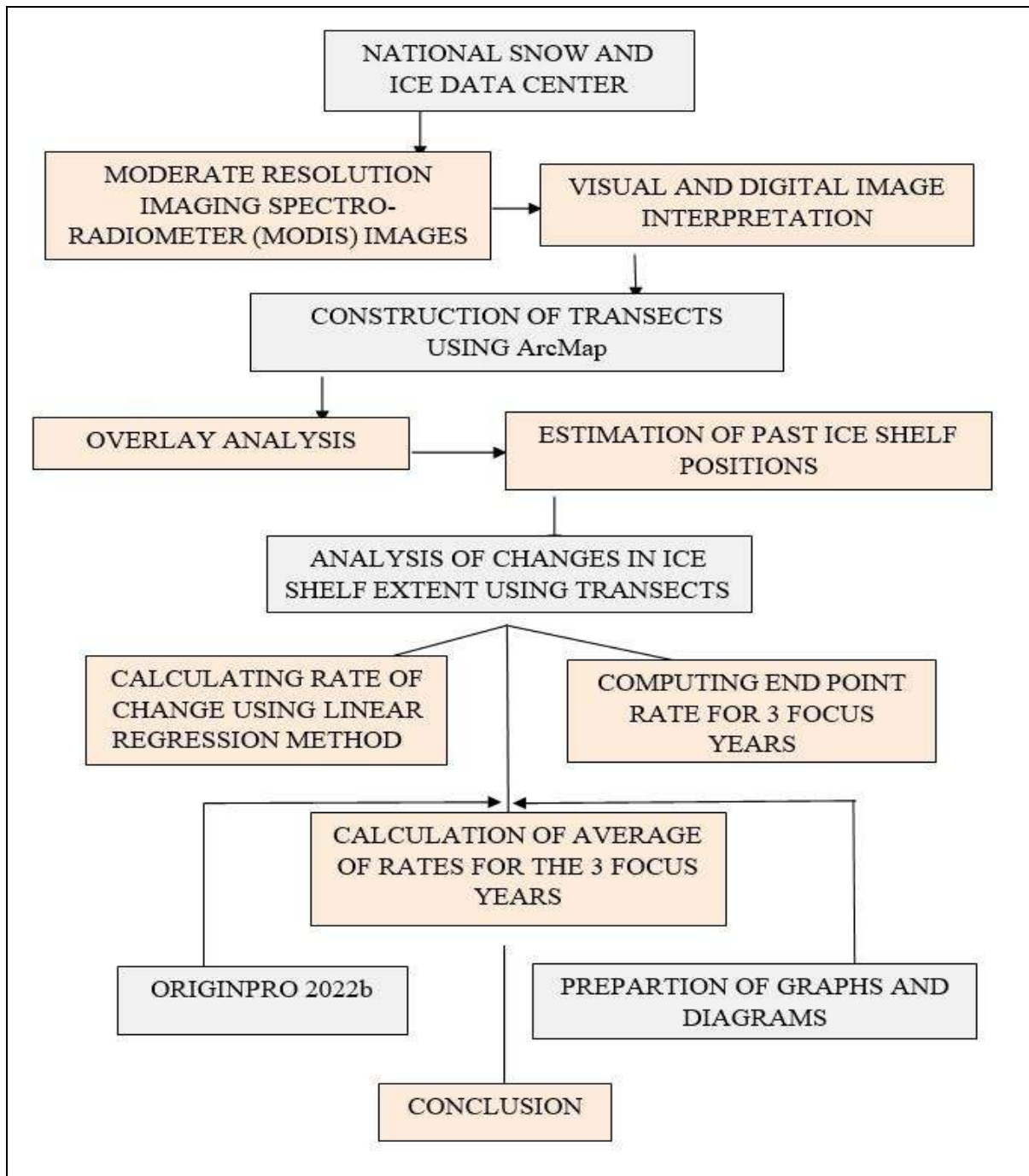


**Fig 3:** Flowchart showing various steps applied in this study

The computed values have been used to prepare graphs and diagrams on OriginPro 2022b software. It has been found out with the help of these graphs and diagrams that net progradation has taken place over the span of 16 years in the Ronne Ice Shelf.

**The three methods used have been discussed in detail below**

**1. End Point Rate:** Short term rates of ice shelf extent changes have been calculated for each transect using this method from the year 2005-2019. The end point rate is calculated by finding out the difference between two survey years (Fenster *et al.*, 1993) <sup>[2]</sup> and dividing it by the time between the survey years which gives a result in metres per year. In this study the EPR has been calculated for each transect TR1 to TR91 from 2005 to 2019 though our focus has been Sector II of the ice shelf.

**2. Average of Rates:** This is a widely used method for calculating the arithmetic mean of the rates. The result is obtained by dividing the total length of each transect divided by the number of years. In this study the AOR has been calculated for the focus years, 2009, 2014 and 2019 in order to find out the change at an interval of 5 years starting from the base year of 2004.

**3. Linear regression:** This method is used for calculating long-term changes in the ice shelf extent in meters per year for each transect in the second sector using the slope calculated in the MS Excel (Allan *et al.*, 2003) <sup>[1]</sup>. The formula used for this method is:

$$y = mx + c$$

where,  $y$  denotes the location of the ice shelf,  $x$  is the year for which the linear regression is being calculated date,  $c$  is the intercept, and  $m$  is the rate at which the ice shelf,

**Results**

In order to understand the change in the pattern of the ice shelf extent morphology various methods have been followed. The change has been studied by using overlay analysis of the digitized ice water lines at an interval of 5 years for 3 different time periods (i.e., 2004-2009, 2010-2014 and 2015-2019).

The entire ice shelf has been divided into transects at an uniform interval of 5 km oriented vertical to the baseline year 2004. The parts of transects cutting the ice water lines between the baseline year and the individual years have been digitized in order to find out the progradation and recession occurring at different transect points. The resultant lengths have further been used to cross validate the rate of change in the extent by using three methods, End Point Rate (EPR), Average of Rates (AOR) and Linear Regression Methods (LR). The transects have been divided into 3 sectors on the basis of the amount of change taking place in

the ice shelf. After dividing the transects into sectors the rate of change has been calculated using three methods mentioned above in MS Excel. The computed results have shown net progradation mainly in the second sector from TR26 to TR91 which varies from 11441.92 m/year to 18161.13 m/year respectively. The ice shelf extents have been studied taking into account changes in the 3 focus years from the base year 2004. For better understanding and visualisation, the lengths of the transects that have shown progradation has been depicted by the green colour lines, while the lines showing recession has been depicted by the colour red. In the above diagram it has been observed that between the years 2004-2005 there has been recession more than progradation across the length of the Ronne Ice Shelf. As observed from the given map, a major part of the beginning of the ice shelf from TR1 to TR16 has shown recession, followed by TR20 to TR23, TR58 to TR77 and finally at the end of the ice shelf from TR122 to almost the end of the ice shelf. Only a visible portion of the ice shelf from TR30 to TR57 has shown progradation followed by TR78 to TR91.

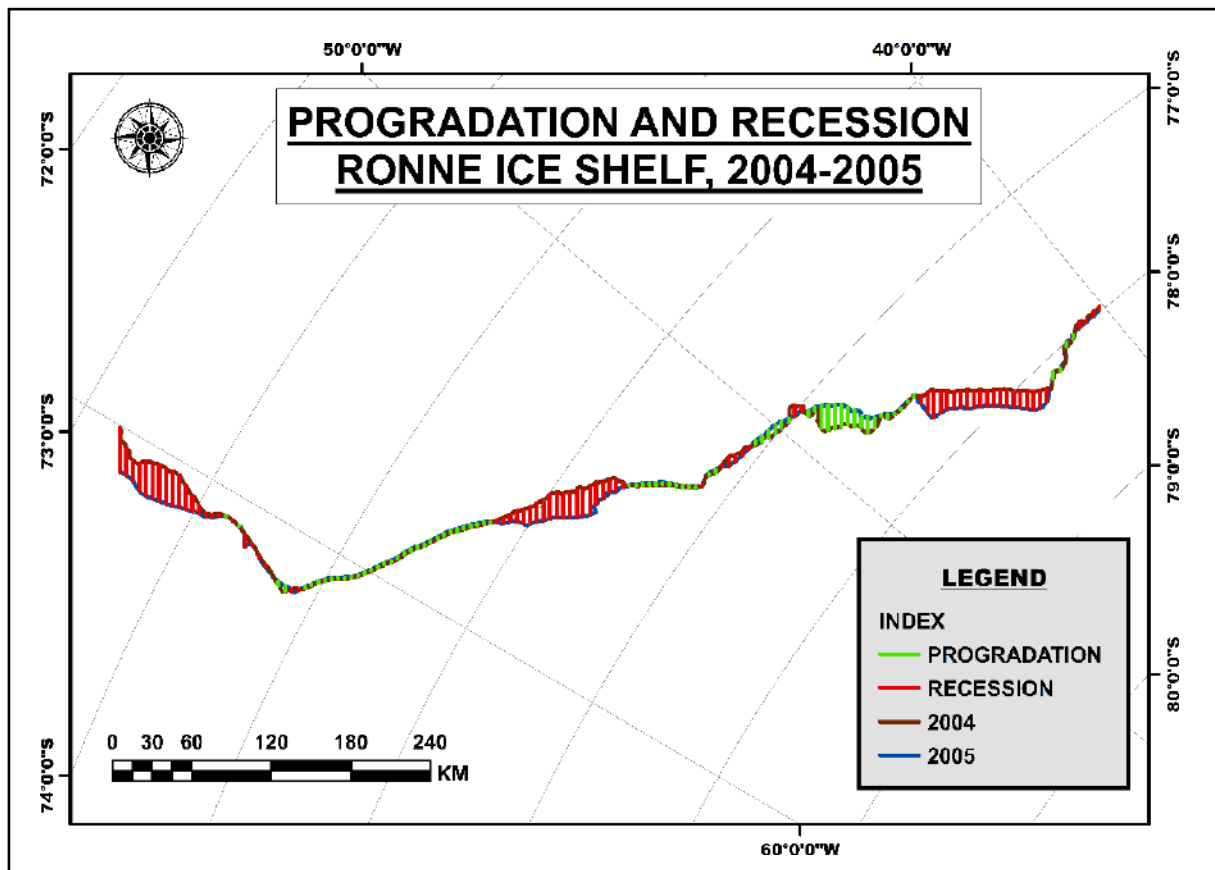


**Fig 4:** Showing the progradation and recession of the Ronne Ice Shelf between 2004 and 2005

It should be noted that with a rise in the effect of global warming, it is quite natural that ice shelves are shrinking due to the rise in temperature which has resulted in its melting, thereby affecting a rise in the sea levels for which these ice shelves are a source of water. The computed

results using the EPR method shows a noticeable change from -32.77 km/year at TR1 to 21.34 km/year at TR91. It must also be noted that the computed values prove that there has not been much of recession of the ice shelf due to the reasons discussed above during the year 2004-2005.

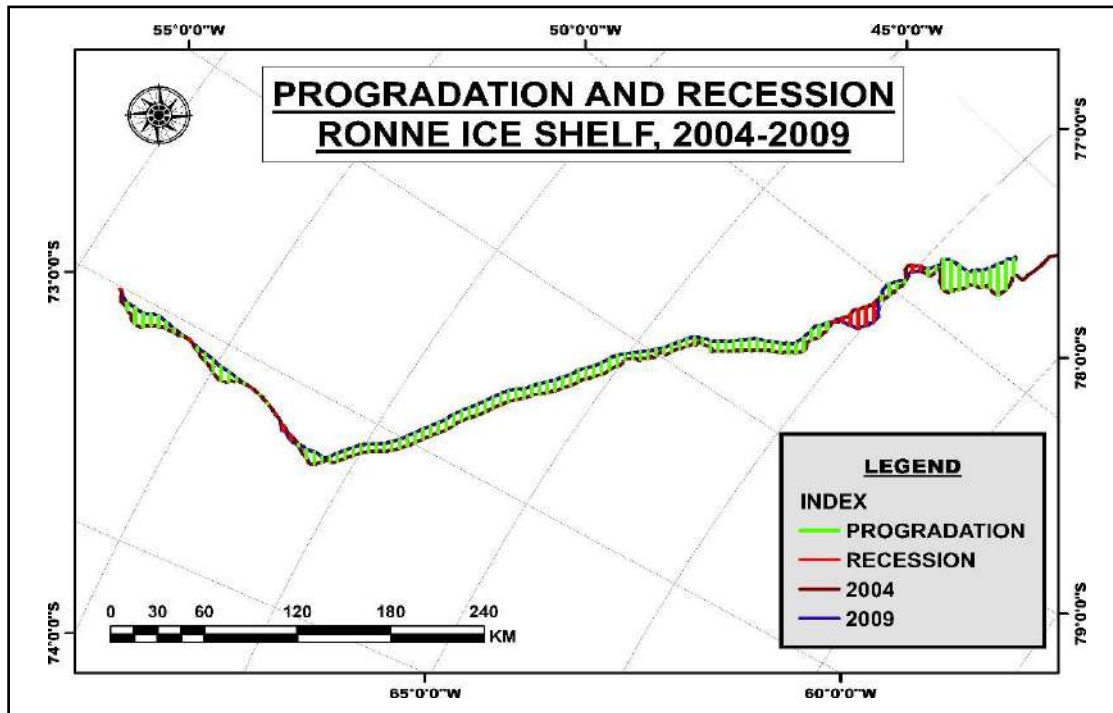


Fig 5: Showing progradation and recession in Ronne Ice Shelf between 2004 and 2009

In the above diagram we can observe a contrary situation as opposed to the change in the ice shelf extent from 2004-2005, wherein a major portion had observed recession more than progradation. From the year 2004-2009 we can majorly observe progradation of the ice shelf across the length with very few transect lengths showing recession. There has been significant advancement in the ice shelf primarily because there have been higher freezing rates as compared to basal melting which has resulted in an observable change in the extent of the RIS.

As observed from the computed results, TR1 to TR116 has shown progradation, the highest being 21.27 km/year at TR114. It has also been found that the computed results from the EPR method have shown a drastic change from -0.013 km/year at TR1 to 1.587 km/year at TR91. Hence, it can be said that there has been major progradation observed by means of the digitised results cross validated by applying the EPR method as well. The Linear Regression method shows a major change in the rate from 6.36 km/year at TR26 to 7.17 km/year at TR91.

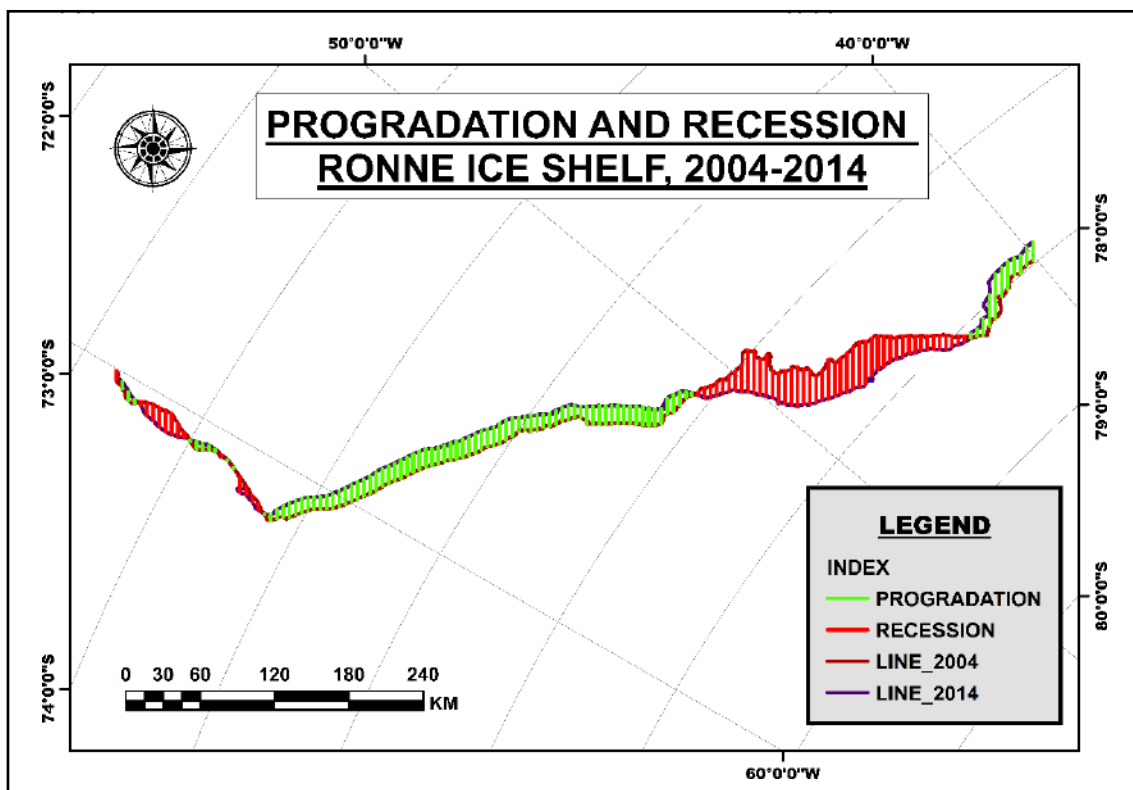


Fig 6: Showing progradation and recession in Ronne Ice shelf between 2004 and 2014

A major difference has been sited between the year 2004-2014 wherein most parts of the ice shelf extent has shown progradation in the western part, with a considerable portion also depicting recession. This has been observed primarily in the eastern parts of the ice shelf wherein the ice shelf has gone through a stage of melting that has resulted in its depletion and has further contributed to a sea level rise in the surrounding areas. The digitised results show that TR26 to TR94 has shown an

increase in the ice shelf which is an outcome of the basal melting point being low and the freezing rates being high. The computed results from the different methods further prove that the ice shelf has undergone a net progradation ranging from -0.71 km/year at TR1 to 1.36 km/year at TR91. It has also been found that the Linear Regression method shows a rate of change 8.899 km/year at TR26 to 12.66 km/year at TR91, which is the second sector, that shows a major progradation across all the years.

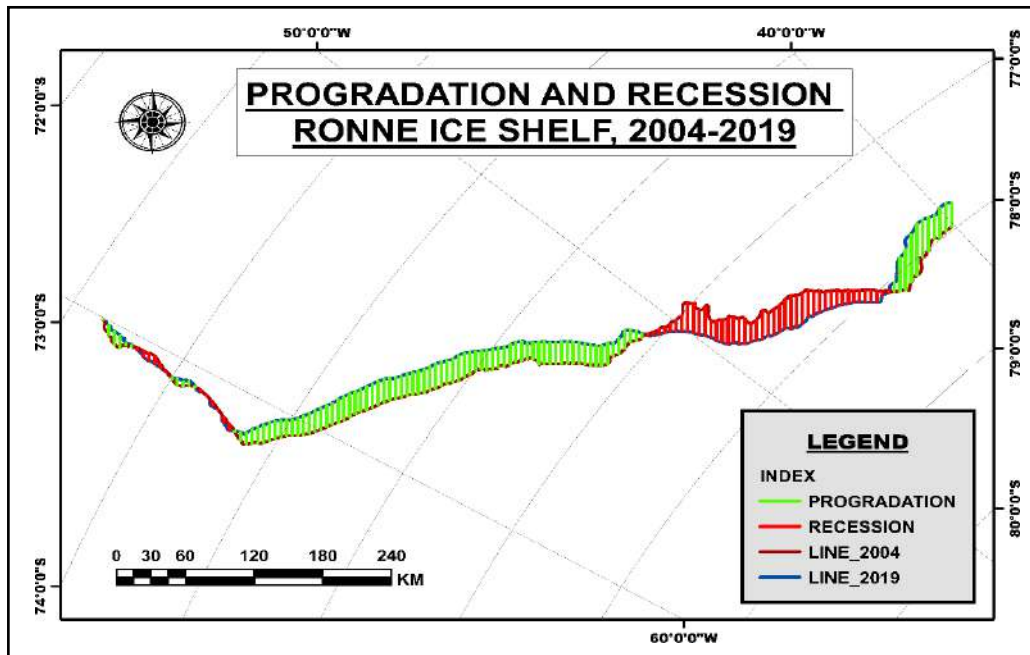


Fig 7: Showing progradation and recession in Ronne Ice Shelf between 2004 and 2019

Finally, the difference between the beginning and the ending years of the study has been analysed. The rate of change observed between these two years is quite similar to Fig 4. As observed from the digitised output a net progradation has been accounted to the second sector that includes the transects between TR23 and TR95. The progradation has

been maximum at TR63 of 24.34 km/year. The calculated EPR shows values ranging from 0.007 km/year at TR1 to 1.004 km/year at TR91. The cross validated results using Linear Regression also shows progradation rate of 11.44 km/year at TR26 to 18.16 km/year at TR91

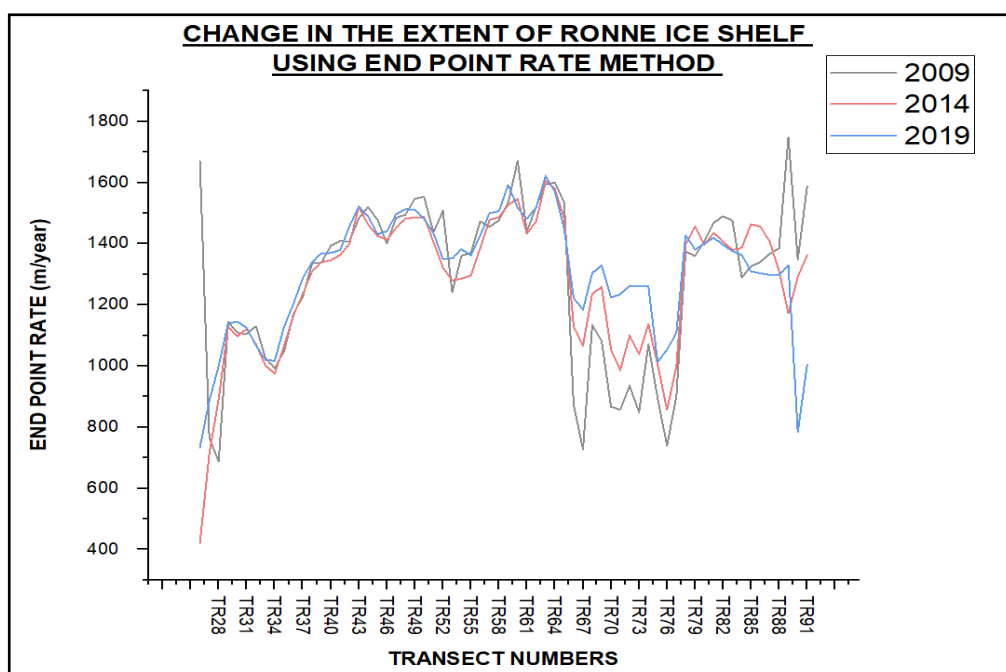
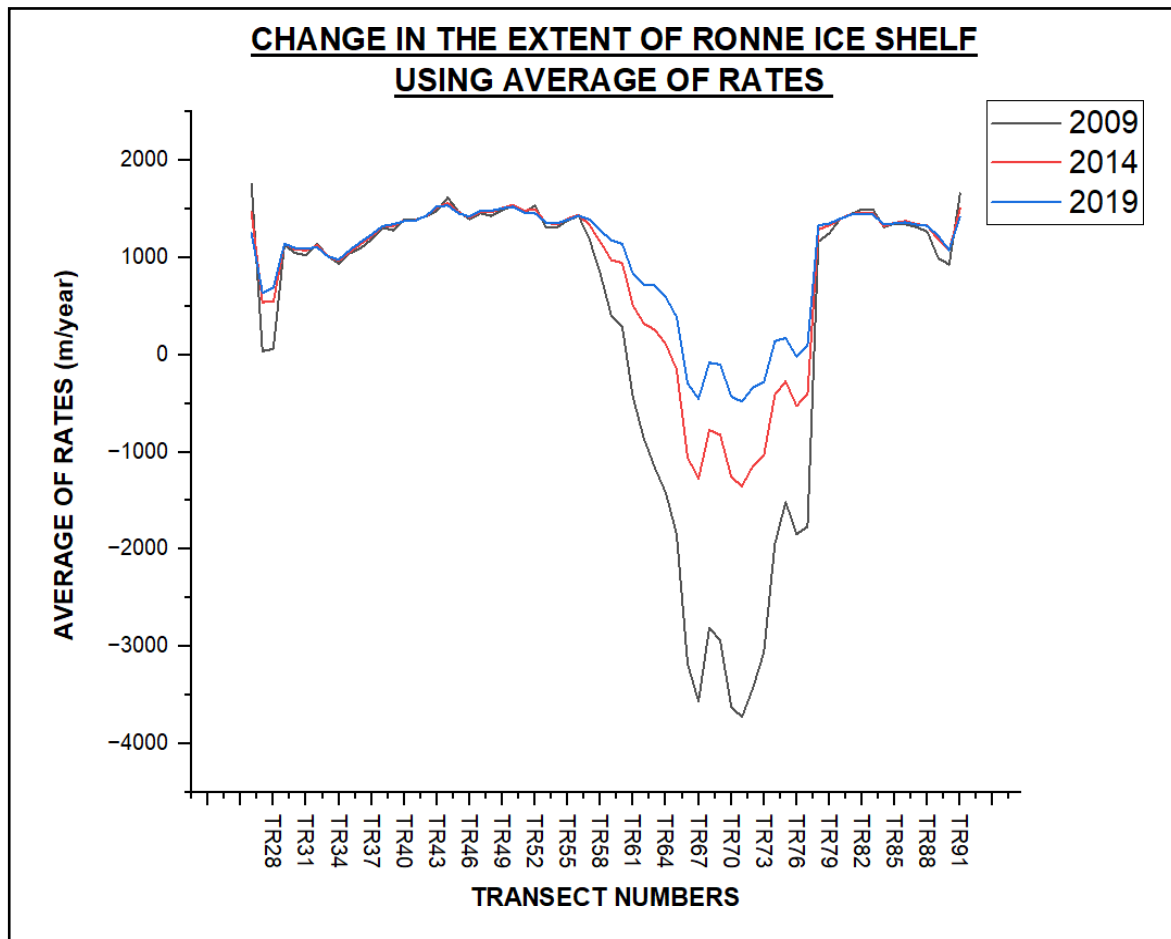


Fig 8: Graph showing the Ronne ice shelf extent change using the EPR method

Hence, it can be said that the Ronne Ice Shelf has primarily undergone progradation at a wide range and shown an increase resulting out of the high freezing rates of the bottom ice waters and also due to the basal melting point being low and ineffective compared to the freezing of the waters.

Figure 7 represents the extent of Ronne Ice Shelf using the End point rate method. This graph represents three focus years that is 2009, 2014 and 2019 which has been prepared for Sector II that is from TR26 to TR91. This section has been particularly selected because it showed the maximum variation in the ice water lines which could be attributed to

bathymetric changes and climate change. It can be observed from the graph that the initial transects that is from TR26 to TR46 almost have identical values that range from 1.1 km/year to 1.4 km/year. After this section we can see slight variations from TR46 to TR64 which alternated in a range from 1.35 km/year to 1.4 km/year. The maximum variation has been observed from TR46 to TR91 where the values are dipping to a great extent that is from 1.3 km/year to 0.7 km/year and there is sudden rise in the value to 1.7 km/year. From the overall graph we can say that the year 2009 has shown a significant amount of variation compared to the years of 2014 and 2019



**Fig 9:** Graph showing the Ronne ice shelf extent change using AOR method

Figure8 represents the extent of Ronne Ice Shelf using the Average of rates method. This graph represents three focus years that is 2009, 2014 and 2019 which was prepared for Sector II that is from TR26 to TR91. This section was particularly selected because it showed the maximum variation in the ice water lines which could be attributed to bathymetric changes and climate change. From the graph we can observe that the year 2009 shows a slight dip in values from TR28 to TR31 where the value ranges from 0.5 km/year to 0.01 km/year. The rest of the years have an

identical moving line where the range is from 0.8 km/year to 1.7 km/year which go from TR26 to TR57. After this there is a sudden variation of values for all three years but the maximum dip in values is seen for the year 2009 where it ranges from 1.3 km/year to - 3.5 km/year. This sudden variation is seen from transect 57 to transect 78 for all the three focus years. Again, from TR78 to TR91 the values are identical for all the three years which range from 1.2 km/year to 1.6 km/year.



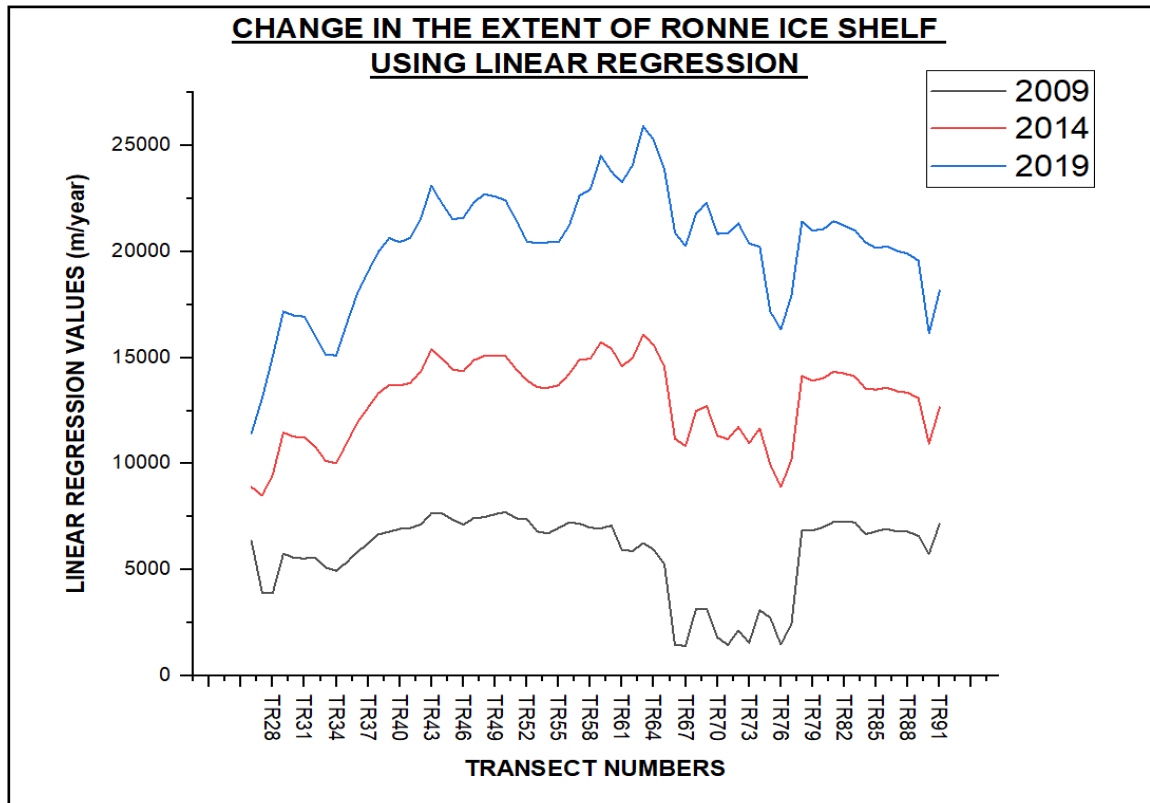


Fig 10: Graph showing the Ronne ice shelf extent change using LR method

Figure 9 represents the extent of Ronne Ice Shelf using the Linear Regression method. This graph represents three focus years that is 2009, 2014 and 2019 which was prepared for Sector II that is from TR26 to TR91. This section was particularly selected because it showed the maximum variation in the ice water lines which could be attributed to bathymetric changes and climate change. From the above graph we can observe that the values are increasing as the years have progressed. To begin with, the year 2009 had a value of 6.3 km/year for transect 26 whereas the year 2014

had the value 8.9 km/year and the year 2019 had the value 11.5 km/year. Through observation we can conclude that the year of 2019 has seen significant variation from TR26 to TR91 where the value ranged from 11.4 km/year to 26 km/year. All the three years have seen a significant dip in values from TR64 to TR77. Here the values for 2019 ranged from 25 km/year to 14 km/year, for the year 2014 it was 15 km/year to 7 km/year whereas the year 2009 showed a range of 6 km/year to 2 km/year.

Table 2: Values for different methods for the three focus years (2009, 2014, 2019) for TR26 to TR91.

Transect No.	EPR			AOR			LR		
	2009	2014	2019	2009	2014	2019	2009	2014	2019
TR26	1670	421	733	1759	1472	1250	6358	8900	11442
TR27	764	714	887	40	544	640	3930	8496	13063
TR28	688	893	1000	61	548	689	3893	9472	15052
TR29	1144	1127	1140	1134	1143	1144	5756	11464	17172
TR30	1110	1098	1145	1048	1086	1101	5553	11274	16995
TR31	1104	1121	1125	1026	1076	1093	5533	11236	16939
TR32	1130	1071	1067	1146	1125	1107	5580	10808	16036
TR33	1026	1002	1020	1016	1017	1015	5104	10129	15155
TR34	994	975	1017	940	969	981	4946	10025	15105
TR35	1048	1066	1129	1047	1060	1077	5351	10983	16614
TR36	1172	1166	1204	1098	1141	1161	5840	11945	18049
TR37	1226	1235	1287	1188	1221	1237	6217	12634	19052
TR38	1337	1310	1341	1310	1320	1325	6670	13338	20006
TR39	1339	1339	1368	1282	1326	1343	6783	13714	20645
TR40	1393	1346	1370	1390	1384	1377	6924	13685	20447
TR41	1409	1364	1380	1387	1386	1384	6959	13808	20658
TR42	1408	1399	1458	1429	1426	1431	7142	14356	21570
TR43	1483	1520	1521	1481	1516	1525	7656	15386	23116
TR44	1520	1463	1490	1618	1563	1539	7667	14969	22270
TR45	1479	1426	1431	1472	1467	1457	7358	14446	21534
TR46	1401	1413	1441	1397	1415	1424	7119	14361	21602
TR47	1485	1452	1497	1457	1474	1479	7434	14876	22319

TR48	1495	1482	1514	1431	1470	1484	7479	15097	22714
TR49	1548	1486	1511	1492	1511	1509	7621	15114	22608
TR50	1553	1487	1482	1531	1543	1526	7722	15074	22427
TR51	1437	1406	1435	1463	1485	1466	7420	14457	21494
TR52	1508	1322	1350	1536	1500	1458	7384	13933	20482
TR53	1241	1280	1352	1312	1360	1364	6799	13601	20403
TR54	1361	1286	1382	1308	1344	1353	6706	13576	20445
TR55	1370	1296	1362	1386	1401	1391	6963	13703	20443
TR56	1474	1386	1427	1429	1442	1432	7224	14225	21226
TR57	1455	1478	1500	1190	1338	1393	7172	14916	22659
TR58	1477	1487	1506	837	1164	1278	6982	14951	22921
TR59	1535	1528	1592	401	976	1184	6950	15734	24518
TR60	1671	1547	1517	293	945	1143	7080	15423	23765
TR61	1440	1432	1482	-438	507	835	5924	14598	23272
TR62	1522	1475	1519	-864	322	724	5883	14985	24087
TR63	1595	1605	1623	-1162	259	715	6247	16083	25919
TR64	1600	1580	1571	-1418	112	597	5948	15606	25263
TR65	1534	1483	1448	-1845	-151	389	5265	14579	23893
TR66	874	1130	1222	-3177	-1054	-293	1431	11163	20895
TR67	728	1067	1185	-3567	-1276	-451	1414	10837	20260
TR68	1133	1237	1305	-2807	-774	-78	3159	12487	21815
TR69	1083	1258	1330	-2939	-821	-100	3152	12722	22293
TR70	867	1054	1224	-3623	-1257	-427	1806	11323	20840
TR71	857	987	1234	-3726	-1349	-481	1448	11160	20872
TR72	936	1100	1263	-3429	-1143	-336	2135	11735	21335
TR73	849	1039	1260	-3060	-1036	-282	1548	10964	20381
TR74	1071	1137	1260	-1948	-410	141	3092	11663	20234
TR75	895	1006	1013	-1514	-273	175	2736	9961	17186
TR76	739	857	1053	-1846	-525	-18	1469	8901	16333
TR77	902	1000	1109	-1769	-403	99	2432	10175	17918
TR78	1375	1397	1428	1165	1292	1334	6842	14131	21419
TR79	1360	1457	1381	1252	1333	1351	6837	13921	21005
TR80	1409	1396	1401	1396	1399	1401	7003	14030	21057
TR81	1468	1436	1419	1448	1450	1443	7256	14345	21434
TR82	1490	1407	1397	1498	1464	1451	7282	14258	21233
TR83	1476	1380	1376	1499	1459	1444	7225	14116	21008
TR84	1290	1386	1363	1313	1328	1342	6666	13551	20436
TR85	1327	1464	1310	1354	1360	1354	6809	13494	20179
TR86	1341	1456	1303	1343	1377	1366	6926	13587	20249
TR87	1367	1406	1298	1315	1346	1341	6795	13417	20040
TR88	1385	1311	1297	1268	1330	1327	6795	13349	19903
TR89	1749	1173	1330	996	1187	1224	6599	13087	19575
TR90	1348	1292	784	930	1074	1077	5743	10947	16152
TR91	1587	1362	1005	1665	1511	1421	7167	12664	18161

## Discussion

The visible range of MODIS satellite images have been used to analyse the changes occurring in the extent of the Ronne Ice Shelf using the End Point Rate, Average of Rates and Linear Regression techniques. The impact of the ocean-climate forcing on the ice shelf has been an important factor that has been investigated taking its linkages with the ice shelf during the austral summer months, mid-February to early March. In order to understand the advancement in the Ronne Ice Shelf since 2004, the relation lying between the ice-mass change and the ocean atmosphere temperature have been investigated carefully. The significant role of the melting and freezing of ice sheets has also been taken into account.

The process of melting of the ice shelves leads to the stratification of the water column due to the top layer cooling and freezing which results in the release salt in the water. The process of ocean circulation underneath the ice shelves are also responsible for the formation of a marine ice layer. Hence, it has been observed that there has been major increase in the ice shelves in the past 15 years. The

rate of recession that has taken place accounts to the effects of rise in temperatures in those areas that has affected the melting of the ice shelves and contributed to the rise in the water levels in the surrounding areas thus resulting in a change in the world climate as a whole.

## Conclusion

This study has revealed that the MODIS satellite images that have been collected for the austral summer months have recorded net progradation or a significant increase in the extent of the Ronne Ice Shelf extent which may be due to ice rise in the eastern side. The change has mainly been observed in the Sector II of the ice shelf from TR26 to TR91, wherein the ice shelves have mostly shown progradation across all the years from 2004 to 2019. Computed results have shown that there has been approximately 20 km increase in the ice shelf between the base year 2004 and the final year 2019 of the concerned period of study. The past ice shelves have also shown recession in a few transects which also helps us understand that the effect of climate change has affected the ice shelves

and caused a retreat, due to which there has been an overall rise in the sea level. The factors contributing to the increase in the ice shelves are mainly the basal melting and high freezing rates in that region. It can be said that any notable change in the sea-ice extent of this region is responsible for affecting the global climate as it accounts for a considerable part of the ice shelves of Antarctica. Since, this ice shelf is the second largest in the continent, it is important for us to employ measures that will help in keeping the ice shelves intact and studies should be conducted in order to understand the changes taking place in this region.

## References

- Allan JC, Komar PD, Priest GR. Shoreline Variability on the High-Energy Oregon Coast and its Usefulness in Erosion-Hazard Assessments. *Journal of Coastal Research*. 2003;38:83-105. <https://doi.org/10.2307/25736601>
- Fenster MS, Dolan R, Elder JF. A new method for predicting shoreline positions from historical data. *Journal of Coastal Research*. 1993;9:147-171.
- Fricker HA, Coleman R, Padman L, Scambos TA, Bohlander J, Brunt KM. Mapping the grounding zone of the Amery Ice Shelf, East Antarctica using InSAR, MODIS and ICESat. *Antarctic Science*. 2009;21:515-532. <https://doi.org/10.1017/S095410200999023X>
- Fricker HA, Young NW, Allison I, Coleman R. Iceberg calving from the Amery Ice Shelf, East Antarctica. *Ann. Glaciol*. 2002;34:241-246. <https://doi.org/10.3189/172756402781817581>
- Hellmer HH, Jacobs SS. Ocean interactions with the base of Amery Ice Shelf, Antarctica. *J. Geophys. Res*. 1992;97(20):305-320. <https://doi.org/10.1029/92JC01856>
- Herrera-Borreguero L, Coleman R, Allison I, Rintoul SR, Craven M, Williams GD. Circulation of modified Circumpolar Deep Water and basal melt beneath the Amery Ice Shelf, East Antarctica. *J. Geophys. Res. Ocean*. 2015;120:3098–3112. <https://doi.org/10.1002/2015JC010697>
- Holland PR, Jenkins A, Holland DM. The response of Ice shelf basal melting to variations in ocean temperature. *Journal of Climate*. 2008;21:2558-2572. <https://doi.org/10.1175/2007JCLI1909.1>
- Joughin I. Ice-sheet velocity mapping: A combined interferometric and speckle-tracking approach. *Annals of Glaciology*. 2002;34:195-201. <https://doi.org/10.3189/172756402781817978>
- King MA, Coleman R, Morgan PJ, Hurd RS. Velocity change of the Amery Ice Shelf, East Antarctica, during the period 1968-1999. *Journal of Geophysical Research: Earth Surface*. 2007;112:1-11. <https://doi.org/10.1029/2006JF000609>
- Rignot E, Jacobs S, Mouginot J, Scheuchl B. Ice Shelf Melting Around Antarctica. *Science*. 2013;1:1-15. <https://doi.org/10.1126/science.1235798>
- Rignot E, MacAyeal DR. Ice-shelf dynamics near the front of the Filchner-Ronne Ice Shelf, Antarctica, revealed by SAR interferometry. *Journal of Glaciology*; c1989. p. 44.
- Swithinbank C, Jr, RSW, Ferrigno JG, Foley KM, Rosanova CE. Coastal-change and glaciological map of the Bakutis Coast, Antarctica; c2003. p. 1972-2002. IMAP. <https://doi.org/10.3133/I2600F>
- Thomson J, Rogers WE. Swell and sea in the emerging Arctic Ocean. *Geophysical Research Letters*. 2014;41:3136–3140. <https://doi.org/10.1002/2014GL059983>
- Walker CC, Bassis JN, Fricker HA, Czerwinski RJ. Observations of interannual and spatial variability in rift propagation in the Amery Ice Shelf, Antarctica, 2002-14. *J. Glaciol*. 2015;61:243–252. <https://doi.org/10.3189/2015JoG14J151>
- Webber BGM, Heywood KJ, Stevens DP, Dutrieux P, Abrahamsen EP, Jenkins A, Jacobs SS, *et al.* Mechanisms driving variability in the ocean forcing of Pine Island Glacier. *Nature Communications* 2017;8(1):1–8. <https://doi.org/10.1038/ncomms14507>
- Wen J, Wang Y, Wang W, Jezek KC, Liu H, Allison I. Basal melting and freezing under the Amery Ice Shelf, East Antarctica. *Journal of Glaciology*. 2010;56:81-90. <https://doi.org/10.3189/002214310791190820>
- Williams, Michael JM, Grosfeld K, Warner RC, Gerdes R. the Amery Ice Shelf , Antarctica Determann; c2001. p. 106.
- Williams, Michael JM, Grosfeld K, Warner RC, Gerdes R, Determann J. Ocean circulation and ice-ocean interaction beneath the Amery Ice Shelf, Antarctica. *Journal of Geophysical Research: Oceans*. 2001;106:22383-22399. <https://doi.org/10.1029/2000jc000236>
- Williams MJM, Warner RC, Budd WF. Sensitivity of the Amery Ice Shelf, Antarctica, to changes in the climate of the southern ocean. *Journal of Climate*. 2002;15:2740-2757. [https://doi.org/10.1175/1520-0442\(2002\)015<2740:SOTAIS>2.0.CO;2](https://doi.org/10.1175/1520-0442(2002)015<2740:SOTAIS>2.0.CO;2)
- Young NW, Hyland G. Velocity and strain rates derived from InSAR analysis over the Amery Ice Shelf, East Antarctica. *Annals of Glaciology*. 2002;34:228-234. <https://doi.org/10.3189/172756402781817842>
- Yu J, Liu H, Jezek KC, Warner RC, Wen J. Analysis of velocity field, mass balance, and basal melt of the Lambert glacier-amery ice shelf system by incorporating Radarsat SAR interferometry and ICE Sat laser altimetry measurements. *Journal of Geophysical Research: Solid Earth*. 2010;115:1-16. <https://doi.org/10.1029/2010JB007456>